Research in Pharmaceutical Sciences, August 2024; 19(4): 475-488
Received: 09-03-2024
Peer Reviewed: 21-05-2024
Revised: 30-06-2024
Accepted: 07-07-2024
Published: 19-08-2024

School of Pharmacy & Pharmaceutical Sciences
Isfahan University of Medical Sciences

Original Article

Bilirubin, once a toxin but now an antioxidant alleviating non-alcoholic fatty liver disease in an autophagy-dependent manner in high-fat diet-induced rats: a molecular and histopathological analysis

Ramin Tavakoli[1,2], Mohammad Hasan Maleki[2], Omid Vakili[3], Motahareh Taghizadeh[2], Fatemeh Zal[2], and Sayed Mohammad Shafiee[4,*]

[1]Student Research Committee, School of Medicine, Shiraz University of Medical Sciences, Shiraz, Iran.
[2]Department of Clinical Biochemistry, School of Medicine, Shiraz University of Medical Sciences, Shiraz, Iran.
[3]Department of Clinical Biochemistry, School of Pharmacy and Pharmaceutical Sciences, Isfahan University of Medical Sciences, Isfahan, Iran.
[4]Autophagy Research Center, Department of Clinical Biochemistry, School of Medicine, Shiraz University of Medical Sciences, Shiraz, Iran.

Abstract

Background and purpose: As an endogenous antioxidant, bilirubin has surprisingly been inversely correlated with the risk of non-alcoholic fatty liver disease (NAFLD). Thereupon, the current evaluation was designed to assess the positive effects of bilirubin on the autophagy flux, as well as the other pathogenic processes and parameters involved in the expansion of NAFLD.
Experimental approach: Thirty adult male rats weighing 150-200 g with free access to sucrose solution (18%) were randomly subdivided into 5 groups (n = 6). Subsequently, the animals were euthanized, and their blood specimens and liver tissue samples were collected to measure serum biochemical indices, liver histopathological changes, intrahepatic triglycerides content, and tissue stereological alterations. Furthermore, the expression levels of autophagy-related genes (Atgs) were measured to assess the state of the autophagy flux.
Findings/Results: Fasting blood glucose, body weight, as well as liver weight, liver-specific enzyme activity, and serum lipid profile indices markedly decreased in rats that underwent a six-week bilirubin treatment compared to the control group. In addition, histopathological studies showed that hepatic steatosis, fibrosis, inflammation, and necrosis significantly decreased in the groups that received bilirubin compared to the control animals. Bilirubin also caused significant alterations in the expression levels of the Atgs, as well as the Beclin-1 protein.
Conclusion and implication: Bilirubin may have potential ameliorative effects on NAFLD-associated liver damage. Moreover, the beneficial effects of bilirubin on intrahepatic lipid accumulation and steatosis were comparable with the group that did not ever receive bilirubin.

Keywords: Autophagy; Bilirubin; Inflammation; Non-alcoholic fatty liver disease.

INTRODUCTION

Non-alcoholic fatty liver disease (NAFLD), as the most common cause of persistent liver disorders, is driven by both genetic and lifestyle factors and globally affects 1 in every 3-4 adults (1,2). NAFLD represents particular circumstances of excessive fat accumulation in the liver, which could be restricted to fatty liver or develop into non-alcoholic steatohepatitis (NASH), and subsequent liver cirrhosis, which may eventually result in hepatocellular carcinoma (3). Parenthetically, NASH is developed once the accumulation of triglycerides (TG) results in the activation of pathways associated with inflammation, oxidative stress, and fibrosis (4).

*Corresponding author: S.M. Shafiee
Tel: +98-7132303029, Fax: +98-7132303029
Email: shafieem@sums.ac.ir

Access this article online
Website: http://rps.mui.ac.ir
DOI: 10.4103/RPS.RPS_53_24

Although the pathogenesis of NAFLD is not completely understood, insulin resistance, dyslipidemia, oxidative stress, and inflammation are considered the underlying mechanisms linked to the malady, and thus NAFLD is identified as the hepatic manifestation of metabolic syndrome (5). Furthermore, NAFLD progression is the result of the disruption of lipid/glucose homeostasis regulated by distinct metabolic pathways, including lipogenesis and gluconeogenesis (6).

Studies on *in vitro* and *in vivo* NAFLD models have shown that several processes, sometimes parallel to each other, can contribute to the progression of liver inflammation and fibrosis from a simple steatosis (7). In this context, autophagy and its regulatory signaling mechanisms, such as the phosphoinositide 3-kinases/protein kinase B/mammalian target of rapamycin (PI3K/Akt/mTOR) pathway, classically interfere with NAFLD development (8). Once the hepatocytes are experiencing NAFLD-related conditions, mTOR is activated and phosphorylates the Unc-51-like kinase 1, which subsequently associates with autophagy-related genes (Atgs), inhibiting autophagosome formation (9,10). Recent advances in understanding the molecular mechanisms involved in autophagy have provided novel insights into the crosstalk between autophagy and NAFLD, as autophagy can significantly stimulate lipid metabolism (11). Moreover, autophagy-mediated destruction of intracellular lipids, called lipophagy, is an alternative flux for lipolysis alongside cytosolic lipolysis (12). To date, more than 30 Atgs have been discovered in yeast that play substantial roles in the initiation and advancement of autophagy, as well as the lipophagy, which almost all of them (*Atg3*, *Atg5*, *Atg6/Beclin-1*, *Atg7*, *Atg8/LC3*, etc.), have well-identified homologs in mammals (13).

Considering the aforementioned pathogenic mechanisms, several therapeutic agents and approaches have been introduced to cure NAFLD but none of them are definitive for disease eradication. However, the ameliorative effects of antioxidants and anti-inflammatory agents, especially with an endogenous origin, have attracted much attention (14).

Bilirubin, as the byproduct of heme catabolism, which was previously considered a toxic agent, is now a well-known endogenous antioxidant with the ability to destroy the peroxyl radicals by donating hydrogen attached to the tetrapyrrole molecule (15). It has been shown that bilirubin prevents the intracellular lipid oxidation (16). A negative correlation between serum bilirubin levels and NAFLD has been observed in multiple syndrome patient populations; for instance, non-toxic hyperbilirubinemic conditions, as seen in Gilbert's syndrome, could markedly reverse the NAFLD and associated injuries (17). More interestingly, it has been proposed that bilirubin can interfere with autophagosome formation by altering the expression of Atgs and thereby affecting autophagy through the NAFLD expansion (18).

Accordingly, in the current study, we used rat model of NAFLD to assess the positive effects of bilirubin on the expression levels of *Atg3*, *Atg5*, *Atg6*, and *Atg7* genes, along with the ATG6 (Beclin-1 protein) to find out more about the correlation between bilirubin, autophagy, and NAFLD. Since NAFLD is accompanied by histopathological changes in the liver, as well as the organ's structural alterations, we also employed histopathological investigations along with stereological methods for a comprehensive analysis of the liver structures and tissue. Moreover, the serum lipid profile of rat models was analyzed, as the animals were treated with a high-fat diet (HFD) for developing NAFLD.

MATERIALS AND METHODS

Preparation of the high-fat emulsion

The high-fat diet used to develop the NAFLD model in rats included fat (77%), carbohydrates (9%), and protein in the form of milk powder (14%) (Table 1). The emulsion was then stored at -20 °C, rigorously mixed, and heated in 37 °C in bain-marie before each experiment (19).

Table 1. The composition of macro-nutrients and caloric content of the high-fat emulsion.

Components of high-fat emulsion	Quantity
Corn oil	400 g
Sucrose	150 g
Total milk powder	80 g
Cholesterol	100 g
Sodium deoxycholate	10 g
Tween 80	36.4 g
Propylene glycol	31.1 g
Vitamin mixture	2.5 g
Cooking salt	10 g
Mineral mixture	1.5 g
Distilled water	300 mL
Total energy	4342 kcal/L

Preparation of unconjugated bilirubin solution

Since bilirubin is normally water-insoluble, we used a specially modified oleic acid to make it injectable (20). In our experiments, it has been found that injecting a daily dose of 10 mg bilirubin per kg of body weight (which is equivalent to 17 µmol/kg/day) was the most effective dosage. This solution was injected intraperitoneally. This dose almost doubled the bilirubin levels in the blood compared to the untreated rats. In a preliminary study, higher doses of bilirubin (20 and 30 mg/kg/day) were also injected. However, after a week, these doses led to more deaths among the rats. Therefore, the dose of 10 mg/kg/day was chosen due to its ability to effectively increase bilirubin levels while keeping the animals healthy. Interestingly, this dose is similar to the amount of bilirubin in the serum samples of people with Gilbert's syndrome. This dose has been previously reported as safe and effective (21,22).

Animals and experimental design

In the current experiment, 30 adult male rats, weighing 150 to 200 g, were obtained from the Animal Breeding Center of Shiraz University of Medical Sciences, Shiraz, Iran. Prior to the treatments, the animals were kept under the standard conditions, including a 12/12 h light/dark cycle, and a temperature of 25 ± 2 ℃ for a week, with open access to water and nutrients. The protected groups were allowed to use 18% sucrose-containing drinking water. All animal experiments were verified by the University Ethics Committee, and conducted according to the criteria for using and caring for animals at Shiraz University of Medical Sciences (Ethics Committee Code: IR.SUMS.AEC.1401.067). The animals were then arbitrarily divided into 5 groups (6 each) as follows: the control group received only food and water; the HFD group (HFD) received HF emulsion for 14 weeks; the treated group (HFD-BR6) received a 6-week bilirubin regimen (10 mg/kg) following the 8th week of 14-week HFD treatment; the protected group (HFD-BR14), which underwent a 14-week bilirubin therapy (10 mg/kg) while receiving HF emulsion; and the bilirubin group (BR14) that received only 10 mg/kg bilirubin for 14 weeks. To confirm the development of NAFLD, the liver of a rat, receiving a 7-week HFD, was autopsied and sent to the pathology laboratory to confirm pathological examinations, and then the treatments were begun. At the end of the experiment, the animals were anesthetized with a mixture of ketamine (100 mg/kg) and xylazine (10 mg/kg). Then, rats were weighed, the livers were removed and collected, and a small amount of them were placed in liquid nitrogen and processed for quantitative real-time polymerase chain reaction (qRT-PCR) analyses, while the remaining were fixed in 10% formalin buffer for stereological and pathological studies. Eventually, the animals were euthanized by placing them in a CO_2 chamber according to the rules of the University's Ethics Committee.

Biochemical evaluations

Once the treatment regimen ended, blood specimens were collected from the animals' hearts and then centrifuged at 2500 rpm for 10 min. Later, the serum was separated for further measurements, including liver function tests, such as alanine aminotransferase (ALT), aspartate aminotransferase (AST), alkaline phosphatase (ALP), total bilirubin (TB), direct bilirubin (DB), total protein (TP), and albumin, as well as the serum lipid profile, *i.e.* total cholesterol (TC), triglycerides (TG), high-density lipoprotein-cholesterol (HDL-C), low-density lipoprotein-cholesterol (LDL-C), plus fasting blood glucose (FBG), and lactate dehydrogenase (LDH). All biochemical indices were measured using the Pars Azmun diagnostic kits (Pars Azmun Co., Iran), based on the manufacturer's procedures.

Table 2. List of primers' sequences.

Gene	Forward primer	Reverse primer
Atg3	GCTCAGTGCTGTGCGATGAAG	AGCCGTGGCGTCTGGTAGTA
Atg5	TGACGCTGGTAACTGACAAAGTG	TGATGTTCCAAGGCAGAGCTGAG
Atg6	CCAGACAGTGTTGTTGCTCCA	CAGGGACTCCAGATACGAGTG
Atg7	GTCTGTCAAGTGCCTGCTGCT	TGCCTCACGGGATTGGAGTAG
β-actin	CCCATCTATGAGGGTTACGC	TTTAATGTCACGCACGATTTC

Gene expression analyses

The relative expression levels of *Atg3*, *Atg5*, *Atg6* (a.k.a. Beclin-1), and *Atg7* were analyzed by the qRT-PCR technique. Briefly, total RNA was extracted from the frozen liver samples by FastPure™ RNA extraction kit (Yekta Tajhiz, Iran) according to the manufacturer's procedure. The reverse transcription was then performed using the cDNA synthesis kit (Yekta Tajhiz, Iran). The primers' sequences (Table 2) were designed using the AlleleID software (version 7.73). All samples were measured in duplicate, and sterile nuclease-free water (ddH_2O) was served as a no-template control (NTC). qRT-PCR was carried out by the QuantStudio™ 3 Real-Time PCR System (ABI Applied Biosystems, USA), using the SYBR Green Amplicon master mix (Yekta Tajhiz, Iran). The relative expression levels of the mRNA transcripts of interest were adjusted against the expression of the internal standard gene, β-actin. Ultimately, relative quantification was performed by the Applied QuantStudio™ Design & Analysis Software. The relative mRNA expression of the genes of interest was eventually calculated by the comparative Ct method ($2^{-\Delta\Delta Ct}$).

Western bolt analysis

In brief, liver tissues were homogenized and then lysed with radioimmunoprecipitation assay (RIPA) lysis buffer (Thermo Fisher Scientific, USA). The concentration of the extracted ATG6 (Beclin-1) protein was determined by the BCA assay. The amount of 10-30 µg of total protein was opted for sodium dodecyl-sulfate polyacrylamide gel electrophoresis (SDS-PAGE) according to the protein type (15% for MW of 60 kDa and lower, and 10% for MW > 60 kDa). The extracted proteins were conveyed onto 0.2 µm nitrocellulose membranes (Bio-Rad, Hercules, CA, USA; #1620112), which then were incubated with primary antibodies Beclin-1 (Beclin-1 (D40C5) Rabbit mAb (#3495) Q14457) and glyceraldehyde 3-phosphate dehydrogenase (GAPDH) (GAPDH (0411) Mouse mAb (#I1517) sc-47724) in the blocking solution (5% fat-free milk) for 12 h, at 4 ℃. Antibodies were utilized in dilutions based on the manufacturer's procedure. Following the incubation with appropriate secondary antibodies (90 min at room temperature), the membranes were incubated with enhanced chemiluminescence (ECL) reagents (Abcam, Cambridge, MA, USA), and then analyzed by the ChemiDoc™ MP imaging system (Bio-Rad, Hercules, CA, USA). Image Lab densitometry software was used to quantify the intensity of blots, and all bands were adjusted to the GAPDH protein expression quantity to correct the negligible deviations in protein loading.

Stereological assessments of the liver structures

First, the liver was weighed and the volume of the liver (V_{liver}) was measured using the immersion method (23). In brief, a normal saline container was located on a scale and weighed. The liver, suspended by thin threads, was then placed deep inside the container. Then, the total volume of the organ in "cm^3" was calculated by subtracting the weight of the container and water inside, from the newly displayed weight, followed by dividing the result by the normal saline's specific gravity (1.0048). Additionally, the tissue shrinkage was estimated before the fixation of the organ in neutral buffered formaldehyde for a week. Isotropic uniform random sections were obtained by applying the Orientator method to the liver tissue. The sections of the plates were embedded in paraffin blocks (with a thickness

of 5 and 25 µm), and then stained with hematoxylin and eosin (H&E) dye. The rate of tissue volumetric shrinkage [d (sh)] was estimated using the following equations (24,25):

$$\text{Shrinkage} = 1 - (AA/AB)^{1.5} \quad (1)$$

where AA and AB were the areas of circular pieces, pre- and post-tissue processing, cutting, and staining, respectively. Each 5-µm sample section was analyzed using a video-microscopy system, consisting of an E-200 microscope (Nikon, Japan) and a computer. 12-15 microscopic fields were then examined in each rat liver sample and scanned equidistantly along the X and Y axes using a stage micrometer at a final magnification of 1440×. The point probe, consisting of 36 points, was superimposed on the image of the tissue section displayed on the monitor, and the volume density (Vv) of hepatic components (*i.e.* hepatocytes and sinusoids) were measured using the point counting method and the following equations:

$$V_V = P_{(component)} / P_{(reference)} \quad (2)$$

$$V_{(component)} = V_{V\,(component)} \times V_{(liver)} \quad (3)$$

where $P_{(component)}$ and $P_{(reference)}$ were the total number of points in the component's profile and the reference space, respectively.

Estimating the number of hepatocytes' nuclei

The abundance of hepatocytes' nuclei was estimated using the optical dissector method at a final magnification of 3500× by employing 25-µm thick sections (26). An E-200 microscope with a high numerical aperture (1.30) oil immersion objective (×40), linked to a video camera, and an MT12 electronic microcator (Heidenhain, Germany) was then utilized (26,27). The unbiased counting frame was used to count the number of the hepatocytes' nuclei and the Kupffer cells with a specific stereology software (Stereolite, SUMS, Iran). The numerical density (N_V) and the total number of the hepatocytes' nuclei, as well as the Kupffer cells, were counted using the following equations:

$$N_V = \Sigma Q^- / (\Sigma A \times h) \times (t / BA) \quad (4)$$

$$N_{(hepatocytes)} = N_V \times V_{(liver)} \times d_{(sh)} \quad (5)$$

in which "∑Q-" explains the total number of the hepatocytes' nuclei focused on the counting frame, "∑A" explains the total areas of unbiased counting frames in all fields (the area of each frame equals 1400 µm), "h" is the height of the dissector (12 µm), "t" is the mean section's thickness of all fields measured with a microcator (20 µm), and "BA" (block advance) is the section's thickness of the microtome set at 25 µm (26,27).

Histopathological investigations

Following euthanasia, liver tissues were carefully dissected and promptly immersed in a 10% neutral buffered formalin solution to preserve cellular morphology. The tissues underwent a meticulous dehydration process using a graded series of ethanol solutions, ensuring the complete removal of water while maintaining tissue integrity. Subsequently, the dehydrated tissues were embedded in paraffin wax, a process that provides firm support for sectioning. This processing prepares the tissues for detailed microscopic examination.

Thin sections, typically 5-µm thick, were obtained using a microtome. These sections facilitated optimal visualization of cellular and tissue architecture under a microscope. The sections were then stained with H&E dye providing a clear distinction between cellular components, highlighting nuclei in blue and cytoplasm and connective tissue elements in shades of pink. Notably, the sections were stained in two distinct batches to ensure staining consistency throughout the analysis.

A precise histological examination was performed by an experienced liver pathologist who was blinded to the experimental procedures. This approach minimizes bias and ensures an objective evaluation of the tissue architecture. The pathologist evaluated the presence and severity of liver steatosis, inflammation, fibrosis, and even necrosis. The severity of these pathological changes was objectively scored using the validated NAFLD activity score (NAS) (28). This scoring system provides a standardized and semi-quantitative approach to assess the degree of liver damage in NAFLD.

Statistical analyses

Numerical data were declared as mean ± SD. The data were statistically evaluated using the one-way analysis of variance (ANOVA) following Tukey's post hoc test for multiple comparisons using the SPSS software (version 24.0) and the GraphPad PRISM Software (version 9.0.0). All results were considered statistically significant at *p*-values < 0.05.

RESULTS

High-fat diet affects the body weight

Following 14 weeks of receiving HFD, the mean body weight of the HFD rats was 354.83 g demonstrating a significant gain compared to the control group (332.16 g) (Fig. 1). Bilirubin therapy almost normalized the body weight in HFD and BR-14 groups. However, the HFD-BR14 and BR14 groups indicated no considerable difference from the control group. Additionally, bilirubin therapy considerably attenuated the body weight in comparison with the HFD group.

Serum biochemical indices

Liver damage-related indices (ALT, AST, ALP, TB, and DB), as well as the serum FBG and lipid profile parameters (TC, TG, and LDL) significantly increased in the HFD group compared to the control group, while the HDL levels indicated a significant decline. In contrast, a significant decrease was detected in FBG, TC, LDL, TG, ALT, AST, ALP, albumin, and LDH levels in both HFD-BR6 and HFD-BR14 groups compared to the HFD rats. Biochemical indices were not significantly different between the BR14 rats and the control group, except for the levels of albumin, TB, and DB, which significantly increased (Table 3).

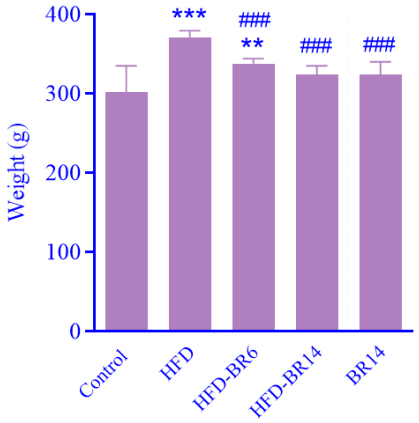

Fig. 1. Mean body weight of rats after 14 weeks of treatment. Normal rats were considered the control group. Values are expressed as mean ± SD. $^{**}P < 0.01$ and $^{***}P < 0.001$ indicate significant differences compared to the control group; $^{###}P < 0.001$ versus the HFD group. HFD, High-fat diet; BR, bilirubin.

Table 3. Effects of bilirubin administration (10 mg/kg/day) on serum biochemical indices. Values are expressed as the mean ± SD. $^{*}P < 0.05$ and $^{***}P < 0.001$ indicate significant differences compared to the control group; $^{##}P < 0.01$, $^{###}P < 0.001$, and $^{###}P < 0.001$ versus the HFD group.

Parameters	Control	HFD	HFD-BR6	HFD-BR14	BR14
FBG (mg/dL)	91.0 ± 6.146	237.0 ± 9.68***	170.0 ± 9.71###	149.5 ± 8.359##	85.5 ± 8.59
TC (mg/dL)	66.78 ± 5.51	125.0 ± 6.13***	91.1 ± 9.85###	69.67 ± 7.20##	58.0 ± 3.66
HDL (mg/dL)	42.67 ± 4.32	34.50 ± 4.50*	37.67 ± 5.08	40.33 ± 2.80	44.17 ± 4.16
LDL (mg/dL)	22.76 ± 4.26	70.71 ± 4.42***	47.44 ± 7.16###	38.67 ± 5.88###	19.38 ± 1.4
TG (mg/dL)	50.22 ± 5.21	96.43 ± 7.65***	76.0 ± 5.63###	63.67 ± 6.21##	46.75 ± 5.31
ALT (IU/L)	31.0 ± 3.08	70.5 ± 5.41***	44.0 ± 6.68###	39.50 ± 3.01###	33.00 ± 5.85
AST (IU/L)	46.6 ± 4.84	104.5 ± 7.86***	78.1 ± 9.57###	61.3 ± 5.98#	4v .5 ± 7.12
ALP(IU/L)	481.7 ± 39.87	820.7 ± 82.67***	593.2 ± 53.78##	572.7 ± 51.02##	491.0 ± 53.94
TP (g/dL)	7.02 ± 0.26	6.987 ± 0.23	6.58 ± 0.21	6.57 ± 0.21	6.64 ± 0.28
Albumin	2.752 ± 0.07	2.782 ± 0.17	2.410 ± 0.10#	2.435 ± 0.13##	2.36 ± 0.12***
TB (mg/dL)	0.096 ± 0.01	0.078 ± 0.01	0.14 ± 0.01###	0.16 ± 0.01###	0.17 ± 0.01***
DB (mg/dL)	0.041 ± 0.01	0.04 ± 0.01	0.08 ± 0.01###	0.08 ± 0.01###	0.08 ± 0.01***
LDH (IU/L)	922.8 ± 66.0	1364 ± 47.3***	1165 ± 136.4##	1122 ± 108.9##	964.5 ± 77.5

HFD, High-fat diet; BR, bilirubin; FBG, Fasting blood glucose; TC, total cholesterol; HDL, high-density lipoprotein; LDL, low-density lipoprotein; TG, triglycerides; ALT, alanine aminotransferase; AST, aspartate aminotransferase; ALP, alkaline phosphatase; TP, total protein; TB, total bilirubin; DB, direct bilirubin; LDH, lactate dehydrogenase

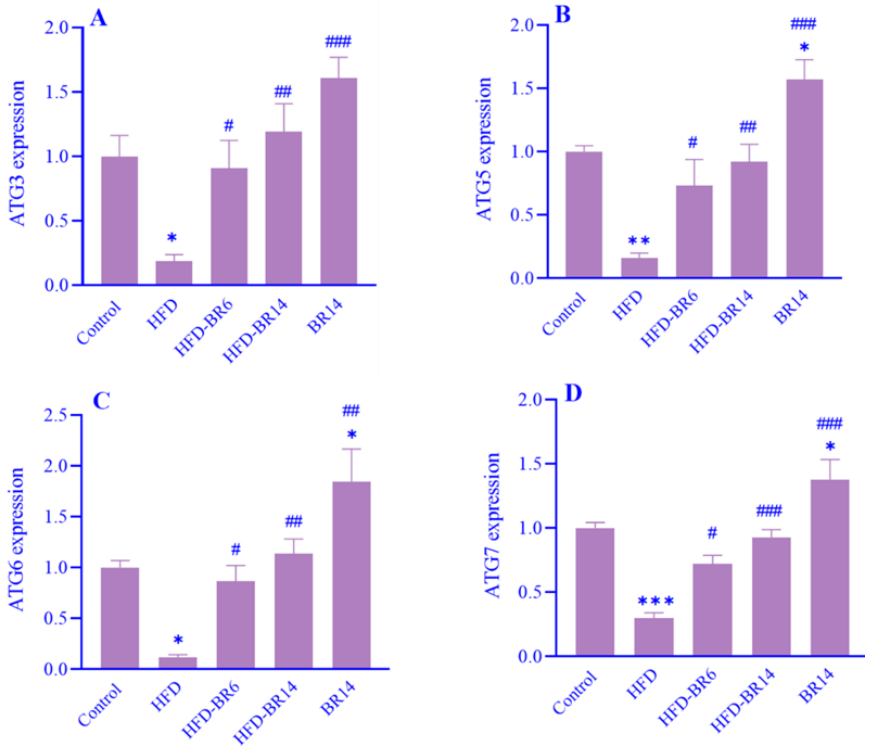

Fig. 2. Comparison of the relative mRNA expression levels of Atgs. Hepatic mRNA expression levels of (A) *Atg3*; (B) *Atg5*; (C) *Atg6*; and (D) *Atg7* were determined by quantitative real-time polymerase chain reaction and normalized to β-actin expression levels. Values are expressed as mean ± SD, n = 6. **P* < 0.05, ***P* < 0.01, and ****P* < 0.001 indicate significant differences compared to the control group; $^{\#}P < 0.05$, $^{\#\#}P < 0.01$, and $^{\#\#\#}P < 0.001$ versus the HFD group. HFD, High-fat diet; BR, bilirubin.

The effect of bilirubin on the expression of autophagy-related genes

A remarkable decrease was found in the mRNA expression levels of hepatic *Atgs*, including *Atg3* (Fig. 2A), *Atg5* (Fig. 2B), *Atg6* (*Beclin-1)* (Fig. 2C), and *Atg7* (Fig. 2D) in the HFD group versus the control group. Still, the animals treated with bilirubin (HFD-BR6, HFD-BR14, and BR14 groups) contrarily experienced a significant rise in the expression levels of the corresponding *Atgs*.

Up-regulated Beclin-1 protein expression, subsequent to the bilirubin administration

Hepatic Beclin-1 protein expression decreased in the HFD group compared to the control group. Bilirubin administration could enhance Beclin-1 and reverse its expression levels to the normal status in both HFD-BR6 and HFD-BR14 groups. Interestingly, the expression levels of Beclin-1 protein demonstrated a notable increase of over twofold following the 14-week treatment period of BR14 rats compared to the control group (Fig. 3A and B).

The effect of bilirubin on the volume of hepatocytes, as well as the hepatic sinusoids

Stereological findings demonstrated that the total volume of the hepatocytes significantly decreased by 15.7% in the HFD group compared to the control group. In the HFD-BR6 group, bilirubin could compensate for the reported decrease in hepatocyte volume by a significant rise of 27% compared to the HFD group. Although the HFD-BR14 group also experienced a decrease in the cell's volume compared to the HFD group (15.7%), it was not statistically significant (Fig. 4A). In the case of sinusoids, the total volume significantly increased by 25% in the HFD group compared to the control group. Bilirubin treatment reduced the increased volume of sinusoids in both HFD-BR6 and HFD-BR14 rats compared to the HFD group in a non-significant manner (Fig. 4B).

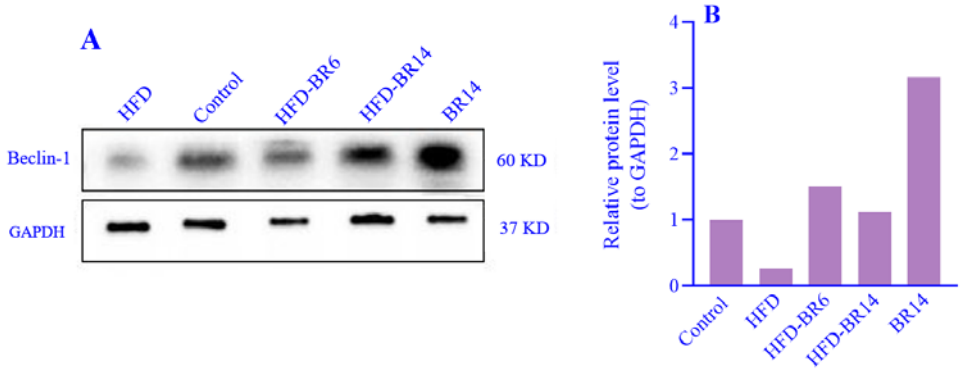

Fig. 3. The effects of bilirubin on Atg6 (Beclin-1) protein expression levels in different rat groups were determined by western blotting and normalized to GAPDH expression levels. (A) Western blot bands; (B) densitometric findings of western blotting analysis. HFD, High-fat diet; BR, bilirubin.

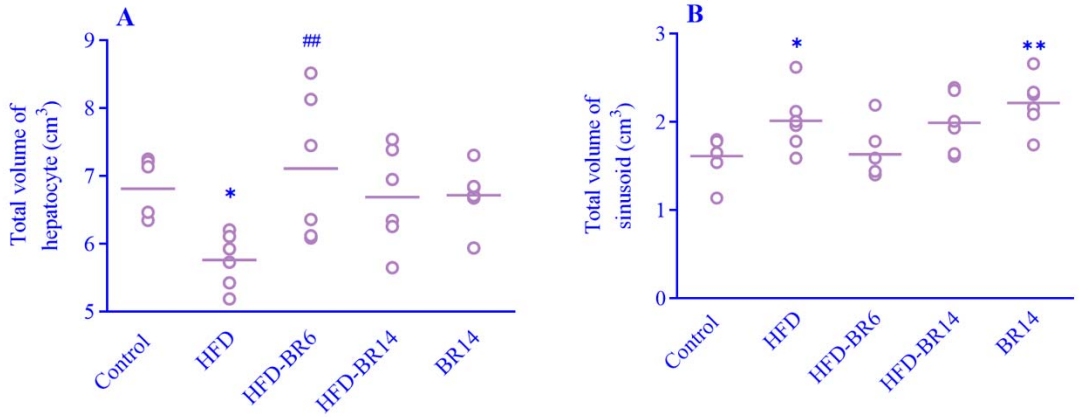

Fig. 4. Volumetric parameters of the liver's structures. (A) Hepatocyte and (B) Sinusoids. Values are expressed as mean ± SD, n = 6. *$P < 0.05$ and **$P < 0.01$ indicate significant differences compared to the control group; $^{\#\#}P < 0.01$ versus the HFD group. HFD, High-fat diet; BR, bilirubin.

The effect of bilirubin on the number of hepatocytes' nuclei, and Kupffer cells

The number of hepatocytes' nuclei represented a decline of 16.74% in the HFD rats compared to the rats of the control group. Treating the HFD rats with 10 mg/kg bilirubin for 6 weeks (HFD-BR6 group) and 14 weeks (HFD-BR14 group) significantly enhanced the number of hepatocytes' nuclei by 20.6% and 22.6%, respectively (Fig. 5A). Moreover, the number of Kupffer cells showed a significant increase (27.34%) in the HFD group in comparison with the control rats. Intriguingly, the above-stated increase was revealed to be notably declined by 18% and 16% in the HFD-BR6 and HFD-BR14 groups, respectively, following receiving bilirubin (Fig. 5B).

Histopathological findings subsequent to bilirubin therapy

As illustrated in both Fig. 6 and Table 4, microscopic examinations of the rats' liver sections from HFD, HFD-BR6, and HFD-BR14 groups demonstrated congestion, hepatic steatosis, inflammation, and large-scale fibrosis (stage 3) in comparison with the liver sections of the rats in the control group that reported no evidence of lipid accumulation, inflammation, or fibrosis. The BR14 group only showed low degrees of inflammation and congestion compared to the control group, possibly due to bilirubin administration and the subsequent liver detoxification processes. The aforementioned outcomes were validated by the H&E staining. Surprisingly, the 6-week bilirubin administration significantly improved steatosis, lobular inflammation, hepatocellular ballooning, and fibrotic lesions.

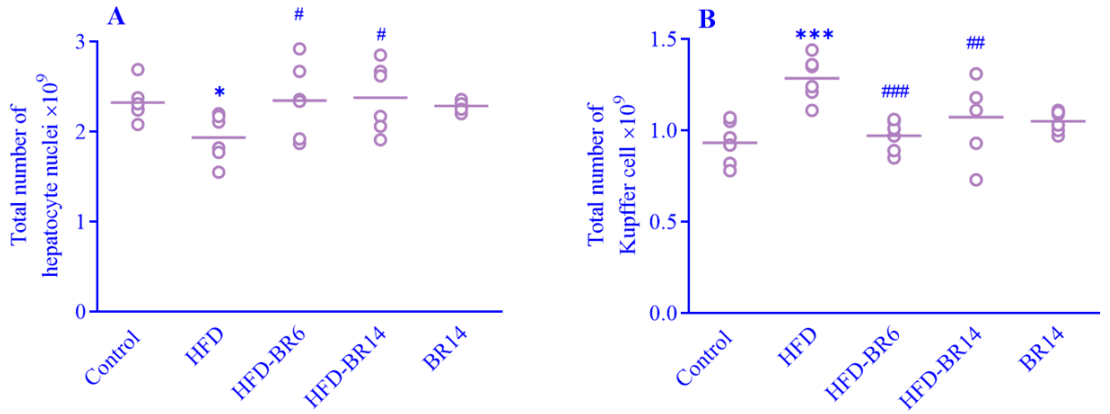

Fig. 5. Evaluation of the quantitative parameters that are responsible for the number of cells and nuclei inside the liver. (A) Hepatocytes' nuclei and (B) Kupffer cells. Values are expressed as mean ± SD, n = 6. *$P < 0.05$ and ***$P < 0.001$ indicate significant differences compared to the control group; $^{\#}P < 0.05$, $^{\#\#}P < 0.01$, and $^{\#\#\#}P < 0.001$ versus the HFD group. HFD, High-fat diet; BR, bilirubin.

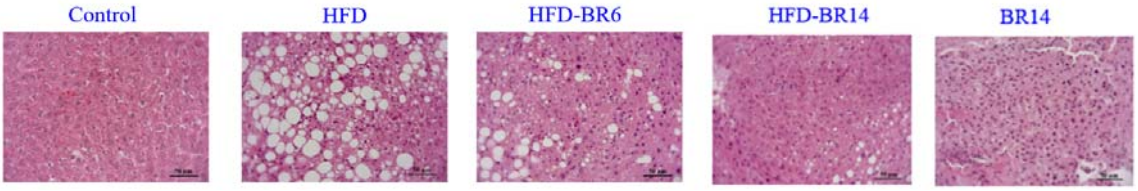

Fig. 6. Histopathological effects of HFD and bilirubin therapy on the liver tissue. Microscopic images (magnification: 40×) of H&E-stained liver tissue sections from HFD, HFD-BR6, and HFD-BR14 groups demonstrate congestion, hepatocellular steatosis, inflammation, and stage 3 fibrosis in comparison with the liver sections of the rats of the control group. BR14 rats only demonstrated low degrees of inflammation and congestion compared to the control group. The steatosis, as well as the lobular inflammation, hepatocellular ballooning, and fibrotic lesions, were found to be improved in rats who received bilirubin (HFD-BR6 and HFD-BR14). Scale bar = 50 µm. HFD, High-fat diet; BR, bilirubin.

Table 4. Histopathological findings of studying the liver tissue. Data are presented as mean ± SD, n = 6. *$P < 0.05$, **$P < 0.01$, and ***$P < 0.001$ indicate significant differences compared to the control group.

Groups	Inflammation	Congestion	Steatosis	Fibrosis
Control	0.21 ± 0.07	0.14 ± 0.06	ND	ND
HFD	1.24 ± 0.40***	1.67 ± 0.34***	3.43 ± 0.60***	1.89 ± 0.30***
HFD-BR6	0.83 ± 0.21***	0.64 ± 0.17*	1.12 ± 0.70**	0.04 ± 0.01**
HFD-BR614	0.32 ± 0.06*	0.21 ± 0.09	0.08 ± 0.01	0.03 ± 0.01*
BR14	0.27 ± 0.30	0.16 ± 0.02	ND	ND

HFD, High-fat diet; BR, bilirubin; ND, not detectable.

DISCUSSION

A few investigations have been conducted to show the antioxidant and anti-inflammatory effects of bilirubin on multiple maladies and pathological conditions (29-31). The discovery of the inverse correlation between non-toxic hyperbilirubinemia seen in Gilbert's syndrome patients and the risk of disease (*e.g.* NAFLD, vascular diseases, malignancies, *etc.*) progression was a milestone that emphasized the significance of bilirubin as an endogenous protective or even therapeutic agent. Recent research indicates that a remarkable reduction in plasma bilirubin level may elevate the risk of NAFLD onset (32). Also, bilirubin levels were demonstrated to be inversely correlated with the risk of NAFLD in a prospective cohort study (33).

Under physiological conditions, lipophagy, as lipolytic autophagy, besides the canonical lipolysis, is responsible for degrading

intrahepatic TG droplets by packaging them inside the autophagosomes to be fused with and digested in lysosomes. Whilst, lipophagy is disrupted during NAFLD, and thereby TG droplets are accumulated in hepatocytes (34). Furthermore, autophagy has also been reported to be in charge of the regulation of liver metabolism, fibrogenesis, and cellular damage (35). It can be concluded that the up-regulation of autophagy could potentially reverse the process of NAFLD progression. Considering the protective and ameliorative potentials of bilirubin, in the current research the effects of bilirubin on autophagy in rat model of NAFLD were assessed and it was noticed that the autophagic flux could be potentiated following the bilirubin administration. Indeed, bilirubin was found to up-modulate the expression of *Atgs*, including *Atg3*, *Atg5*, *Atg6*, and *Atg7*. In this experiment, the NAFLD model was developed by treating rats with HFD resulted in obesity and down-regulation of hepatic autophagy. The observed decrease in autophagy activity is believed to be the consequence of obesity-induced elevation of the calcium-dependent protease calpain 2 that leads to under-expression of *Atgs* and subsequent defects in the autophagic flux. Desirably, acute inhibition of calpain can restore the expression of *Atgs* (36). In addition, the autophagy inhibitor, mTOR, is hyper-activated in obese livers, possibly as a result of the increased amino acid concentrations following HF feeding (37,38). Whilst, in the presence of rapamycin, an autophagy stimulator, a remarkable decrease in the content of TG droplets might be observed (39). The down-regulation of *Atgs*, such as *Atg5*, also reduces the levels of β-hydroxybutyrate that reflects the suppression of β-oxidation, thereby provoking hepatic steatosis (40). Consistently, our findings also confirmed that HFD led to autophagy suppression in rats, resulting in deceleration of intrahepatic lipid degradation. Here is evidence that abnormally increased intracellular TG is inversely correlated with autophagic clearance, as we observed the down-expression of the *Atgs*.

Regarding the substantial role of *Atg6* in triggering the autophagy flux, its protein expression, i.e. Beclin-1, was also investigated in this study in NAFLD rats. Beclin-1 is essential for the localization of autophagic proteins to pre-autophagosomal structures. Several studies have indicated that Beclin-1 regulates autophagy and membrane trafficking, which are involved in a significant number of physiological and pathological processes (41). Western blot analysis of Beclin-1 protein expression revealed a remarkable down-regulation in HFD rats, in which bilirubin administration reversed its expression to normal levels. Interestingly, bilirubin therapy in healthy rats led to a noticeable increase in Beclin-1 protein expression. It can be concluded that bilirubin might trigger the initializing process of autophagy in those with higher circulating bilirubin levels, providing a kind of protection against multiple diseases.

In the present research, it has been demonstrated that bilirubin had positive effects in ameliorating the NAFLD in the groups that received bilirubin compared to the HFD group through increasing the *Atgs* expression levels. Bilirubin as a dual *Atg* agonist, seems to be a desirable alleviator in this situation (12). Indeed, bilirubin enhances the autophagic function primarily by inhibiting the mTOR pathway and decreasing the severity of NAFLD (42). The agonists of *Atgs* can improve insulin resistance, hepatic steatosis, oxidative stress, inflammation, and fibrosis (9). Beyond the autophagy-related effects of bilirubin, it principally modulates the expression of lipid metabolism-related genes, triggers glucose uptake in adipose tissue, and stimulates the differentiation of adipocytes (43). Bilirubin has also been previously shown to directly target the peroxisome proliferator-activated receptor-alpha (PPAR-α), the known regulator of fatty acid β-oxidation. Pathological and biochemical findings also confirmed the above-mentioned outcomes of improving the fatty liver, as indices, such as serum FBG and lipid profile, except for HDL, decreased following 6 weeks of bilirubin treatment. It can be justified by the previously-mentioned role of autophagy in the regulation of lipid content, that its inhibition increases the serum lipid profile, as evidence for the involvement of autophagy in the hepatocytes' lipid digestion system (12). In detail, the administration of bilirubin, most

likely by activating the autophagic flux, reduced the plasma levels of TG, TC, and LDL-C, with no effect on HDL-C content. We also demonstrated that a 6-week bilirubin therapy could significantly improve the liver function indices compared to the HFD group that did not receive bilirubin. In this regard, the positive effects of bilirubin were seen to be more efficient in the HFD-BR14 group than in the HFD-BR6 group but were not significant in the group that received only bilirubin (*i.e.* BR14 group) compared to the control rats. Based on the current findings, 10 mg/kg bilirubin normalized body weight and improved glycemic index in NAFLD rats.

The effects of bilirubin on histopathological changes in the liver of NAFLD rats were also evaluated in this study to confirm the gene expression findings. The congestion, grade III hepatocellular steatosis, inflammation, and extensive fibrosis observed in NAFLD rats compared to the control rats, were consistent with the findings of the study conducted by Xu *et al*. (44); as they found that HFD could result in liver inflammation and fibrosis in rat models. Necroinflammatory grades of NASH have been classified as grade 1 (mild), grade 2 (moderate), and grade 3 (severe) based on the degree of hepatocellular steatosis, ballooning and disarray, and inflammation (intralobular and portal). The NASH Clinical Research Network (NASH CRN) later subclassified stage 1 into 3 categories of NAFLD activity score (NAS) for use in clinical research. The score is calculated as the unweighted sum of the scores for steatosis (0-3), lobular inflammation (0-3), and ballooning (0-2), and ranges from 0 to 8 (45). In the following, we realized that a 6-week bilirubin administration significantly improved the corresponding steatosis, lobular inflammation, hepatocellular ballooning, and fibrotic lesions. This valuable result was in line with findings published by Salomone *et al*. demonstrating low bilirubin levels as independent predictors of advanced inflammation and fibrosis in NASH patients (46). In other words, bilirubin provides antioxidant protection against the development of liver injury from NAFLD to NASH.

To support the results of the gene expression, stereological indices, such as the absolute volume of sinusoids, were also measured, and it was found that the HFD group suffered from sinusoids with increased volumes. At the same time, this expansion was moderated in HFD-BR6 and HFD-BR14 groups that had received bilirubin. It was a substantial finding in our study since the sinusoids are critically responsible for regulating the blood flow to the hepatocytes, especially during hepatic regeneration (47). Regarding the presence of macrophages in the vessels, liver sinusoids are known as micro-vessels that particularly differ from capillaries of other organs (48). Summarily, the long-term treatment of rats with HFD led to detrimental effects on the hepatocytes and hepatic sinusoids. The long-term administration of bilirubin decreased the hepatic lipid accumulation by diminishing hepatic sinusoids and hepatocytes. As the disease progresses, inflammation is exacerbated and the surface activity develops by hepatocyte necrosis at the portal-lobular interface. Acute liver failure is often accompanied by marked hepatocellular degeneration and parenchymal collapse, typically in the form of cirrhosis. Parenchymal apoptosis of hepatocytes is also a prominent feature, seen in the same circumstances (49,50). In this experiment, we observed a significant decrease in the volume and the number of hepatocytes, along with an elevation in the number of Kupffer cells. Notwithstanding, further *in vivo* and observational evaluations, as well as randomized clinical trials, are needed to verify the current findings and the other potential effects of bilirubin on NAFLD onset and progression.

CONCLUSION

Our outcomes suggest that bilirubin has the potential of ameliorating NAFLD in HFD-induced rats, principally through the induction of *Atgs* expression, thus provoking the autophagic flux. The triggered autophagy then stimulates the autophagosome-lysosomal degradation of intrahepatic fat droplets. Furthermore, the corresponding endogenous antioxidant, *i.e*. bilirubin, can desirably reverse the congestion, inflammation, and fibrosis developed in NAFLD livers. The absolute volume of sinusoids and the total number of hepatocytes' nuclei and Kuppfer cells, as well

as the serum biochemical parameters and liver function indices of NAFLD rats, can also be positively affected by bilirubin. Altogether, bilirubin can be considered a potential endogenous protective/therapeutic agent to decrease the risk of NAFLD or decelerate its progression.

Acknowledgments

The current study has been extracted from a Ph.D thesis carried out by R. Tavakoli and was financially supported by the Vice-Chancellor for Research Affairs of Shiraz University of Medical Sciences, Shiraz, Iran through Grant No. 24722.

Conflict of interest statement

The authors declared no conflict of interest in this study.

Authors' contributions

All authors contributed to the study's conception and design. Material preparation, data collection, and analyses were performed by R. Tavakoli, M.H. Maleki, O. Vakili, M. Taghizadeh, and F. Zal. The first draft of the manuscript was written by R. Tavakoli and then was edited and improved by O. Vakili and S.M. Shafiee. Supervision and project administration were conducted by S.M. Shafiee. The finalized article was read and approved by all authors.

REFERENCES

1. El-Din SHS, El-Lakkany NM, El-Naggar AA, Hammam OA, Abd El-Latif HA, Ain-Shoka AA, *et al*. Effects of rosuvastatin and/or β-carotene on non-alcoholic fatty liver in rats. Res Pharm Sci. 2015;10(4):275-287. PMID: 26600855.
2. El-Lakkany NM, Seif El-Din SH, Sabra AA, Hammam OA, Ebeid FA. Co-administration of metformin and N-acetylcysteine with dietary control improves the biochemical and histological manifestations in rats with non-alcoholic fatty liver. Res Pharm Sci. 2016;11(5):374-382. DOI: 10.4103/1735-5362.192487.
3. Hamidi-Zad Z, Moslehi A, Rastegarpanah M. Attenuating effects of allantoin on oxidative stress in a mouse model of nonalcoholic steatohepatitis: role of SIRT1/Nrf2 pathway. Res Pharm Sci. 2021;16(6):651-659. DOI: 10.4103/1735-5362.327511.
4. Naik A, Kosir R, Rozman D. Genomic aspects of NAFLD pathogenesis. Genomics. 2013;102(2):84-95. DOI: 10.1016/j.ygeno.2013.03.007.
5. Sadeghinejad S, Mousavi M, Zeidooni L, Mansouri E, Mohtadi S, Khodayar MJ. Ameliorative effects of umbelliferone against acetaminophen-induced hepatic oxidative stress and inflammation in mice. Res Pharm Sci. 2024;19(1):83-92. DOI: 10.4103/1735-5362.394823.
6. Xu J, Cao K, Li Y, Zou X, Chen C, Szeto IM, *et al*. Bitter gourd inhibits the development of obesity-associated fatty liver in C57BL/6 mice fed a high-fat diet. J Nutr. 2014;144(4):475-483. DOI: 10.3945/jn.113.187450.
7. Eliades M, Spyrou E. Vitamin D: a new player in non-alcoholic fatty liver disease? World J Gastroenterol. 2015;21(6):1718-1727. DOI: 10.3748/wjg.v21.i6.1718.
8. Shintani T, Klionsky DJ. Autophagy in health and disease: a double-edged sword. Science. 2004;306(5698):990-995. DOI: 10.1126/science.1099993.
9. Rautou PE, Mansouri A, Lebrec D, Durand F, Valla D, Moreau R. Autophagy in liver diseases. J Hepatol. 2010;53(6):1123-1134. DOI: 10.1016/j.jhep.2010.07.006.
10. Mizushima N, Yoshimori T, Ohsumi Y. The role of Atg proteins in autophagosome formation. Annu Rev Cell Dev Biol. 2011;27:107-132. DOI: 10.1146/annurev-cellbio-092910-154005.
11. Sinha RA, Farah BL, Singh BK, Siddique MM, Li Y, Wu Y, *et al*. Caffeine stimulates hepatic lipid metabolism by the autophagy-lysosomal pathway in mice. Hepatology. 2014;59(4):1366-1380. DOI: 10.1002/hep.26667.
12. Singh R, Kaushik S, Wang Y, Xiang Y, Novak I, Komatsu M, *et al*. Autophagy regulates lipid metabolism. Nature. 2009;458(7242):1131-1135. DOI: 10.1038/nature07976.
13. Mizushima N, Yoshimori T, Levine B. Methods in mammalian autophagy research. Cell. 2010;140(3): 313-326. DOI: 10.1016/j.cell.2010.01.028.
14. Hinds TD, Jr., Creeden JF, Gordon DM, Stec DF, Donald MC, Stec DE. Bilirubin nanoparticles reduce diet-induced hepatic steatosis, improve fat utilization, and increase plasma beta-hydroxybutyrate. Front Pharmacol. 2020;11:594574. DOI: 10.3389/fphar.2020.594574.
15. Stocker R, Glazer AN, Ames BN. Antioxidant activity of albumin-bound bilirubin. Proc Natl Acad Sci U S A. 1987;84(16):5918-5922. DOI: 10.1073/pnas.84.16.5918.
16. Wu TW, Fung KP, Yang CC. Unconjugated bilirubin inhibits the oxidation of human low density lipoprotein better than Trolox. Life Sci. 1994;54(25):PL477-PL481. DOI: 10.1016/0024-3205(94)90140-6.
17. Landerer S, Kalthoff S, Paulusch S, Strassburg CP. A Gilbert syndrome-associated haplotype protects against fatty liver disease in humanized transgenic mice. Sci Rep. 2020;10(1):8689,1-8. DOI: 10.1038/s41598-020-65481-4.

18. Mao Y, Cheng J, Yu F, Li H, Guo C, Fan X. Ghrelin attenuated lipotoxicity via autophagy induction and nuclear factor-kappaB inhibition. Cell Physiol Biochem. 2015;37(2):563-576. DOI: 10.1159/000430377.
19. Zou Y, Li J, Lu C, Wang J, Ge J, Huang Y, *et al*. High-fat emulsion-induced rat model of nonalcoholic steatohepatitis. Life Sci. 2006;79(11):1100-1107. DOI: 10.1016/j.lfs.2006.03.021.
20. Orio L, Alen F, Pavon FJ, Serrano A, Garcia-Bueno B. Oleoylethanolamide, neuroinflammation, and alcohol abuse. Front Mol Neurosci. 2018;11:490,1-21. DOI: 10.3389/fnmol.2018.00490.
21. Adin CA. Bilirubin as a therapeutic molecule: challenges and opportunities. Antioxidants (Basel). 2021;10(10):1536,1-16. DOI: 10.3390/antiox10101536.
22. Lin JP, O'Donnell CJ, Schwaiger JP, Cupples LA, Lingenhel A, Hunt SC, *et al*. Association between the UGT1A1* 28 allele, bilirubin levels, and coronary heart disease in the Framingham Heart Study. Circulation. 2006;114(14):1476-1481. DOI: 10.1161/CIRCULATIONAHA.106.633206.
23. Altunkaynak BZ, Ozbek E. Overweight and structural alterations of the liver in female rats fed a high-fat diet: a stereological and histological study. Turk J Gastroenterol. 2009;20(2):93-103. PMID: 19530041.
24. Karbalay-Doust S, Noorafshan A. Stereological study of the effects of nandrolone decanoate on the mouse liver. Micron. 2009;40(4):471-475. DOI: 10.1016/j.micron.2008.12.006.
25. Marcos R, Monteiro RA, Rocha E. The use of design-based stereology to evaluate volumes and numbers in the liver: a review with practical guidelines. J Anat. 2012;220(4):303-317. DOI: 10.1111/j.1469-7580.2012.01475.x.
26. Namavar MR, Ghalavandi M, Bahmanpour S. The effect of glutathione and buserelin on the stereological parameters of the hypothalamus in the cyclophosphamide-treated mice. J Chem Neuroanat. 2020;110:101871,1-8. DOI: 10.1016/j.jchemneu.2020.101871.
27. von Bartheld CS. Distribution of particles in the z-axis of tissue sections: relevance for counting methods. Neuroquantology. 2011;10(1):66-75. PMID: 23874137.
28. Liang W, Menke AL, Driessen A, Koek GH, Lindeman JH, Stoop R, *et al*. Establishment of a general NAFLD scoring system for rodent models and comparison to human liver pathology. PLoS One. 2014;9(12):e115922,1-17. DOI: 10.1371/journal.pone.0115922.
29. Vakili O, Borji M, Saffari-Chaleshtori J, Shafiee SM. Ameliorative effects of bilirubin on cell culture model of non-alcoholic fatty liver disease. Mol Biol Rep. 2023;50(5):4411-4422. DOI: 10.1007/s11033-023-08339-y.
30. Maleki MH, Nadimi E, Vakili O, Tavakoli R, Taghizadeh M, Dehghanian A, *et al*. Bilirubin improves renal function by reversing the endoplasmic reticulum stress and inflammation in the kidneys of type 2 diabetic rats fed high-fat diet. Chem Biol Interact. 2023;378:110490. DOI: 10.1016/j.cbi.2023.110490.
31. Niknam M, Maleki MH, Khakshournia S, Rasouli M, Vakili O, Shafiee SM. Bilirubin, an endogenous antioxidant that affects p53 protein and its downstream apoptosis/autophagy-related genes in LS180 and SW480 cell culture models of colorectal cancer. Biochem Biophys Res Commun. 2023;672:161-167. DOI: 10.1016/j.bbrc.2023.06.050.
32. Novak P, Jackson AO, Zhao GJ, Yin K. Bilirubin in metabolic syndrome and associated inflammatory diseases: new perspectives. Life Sci. 2020;257:118032,1-6. DOI: 10.1016/j.lfs.2020.118032.
33. Tian J, Zhong R, Liu C, Tang Y, Gong J, Chang J, *et al*. Association between bilirubin and risk of non-alcoholic fatty liver disease based on a prospective cohort study. Sci Rep. 2016;6(1):31006,1-9. DOI: 10.1038/srep31006.
34. Wu B, Wu Y, Tang W. Heme catabolic pathway in inflammation and immune disorders. Front Pharmacol. 2019;10:825,1-15. DOI: 10.3389/fphar.2019.00825.
35. Stec DE, John K, Trabbic CJ, Luniwal A, Hankins MW, Baum J, *et al*. Bilirubin binding to PPARα inhibits lipid accumulation. PLoS One. 2016;11(4):e0153427,1-17. DOI: 10.1371/journal.pone.0153427.
36. Yang L, Li P, Fu S, Calay ES, Hotamisligil GS. Defective hepatic autophagy in obesity promotes ER stress and causes insulin resistance. Cell Metab. 2010;11(6):467-478. DOI: 10.1016/j.cmet.2010.04.005.
37. Codogno P, Meijer AJ. Autophagy: a potential link between obesity and insulin resistance. Cell Metab. 2010;11(6):449-451. DOI: 10.1016/j.cmet.2010.05.006.
38. Newgard CB, An J, Bain JR, Muehlbauer MJ, Stevens RD, Lien LF, *et al*. A branched-chain amino acid-related metabolic signature that differentiates obese and lean humans and contributes to insulin resistance. Cell Metab. 2009;9(4):311-326. DOI: 10.1016/j.cmet.2009.02.002.
39. Zhang X, Deng Y, Xiang J, Liu H, Zhang J, Liao J, *et al*. Galangin improved non-alcoholic fatty liver disease in mice by promoting autophagy. Drug Des Devel Ther. 2020;14:3393-3405. DOI: 10.2147/DDDT.S258187.
40. Sinha RA, Rajak S, Singh BK, Yen PM. Hepatic lipid catabolism via PPAR alpha-lysosomal crosstalk. Int J Mol Sci. 2020;21(7):2391,1-13. DOI: 10.3390/ijms21072391.
41. Kaur S, Changotra H. The beclin 1 interactome: modification and roles in the pathology of autophagy-related disorders. Biochimie. 2020;175:34-49. DOI: 10.1016/j.biochi.2020.04.025.
42. Mehrpour M, Esclatine A, Beau I, Codogno P. Overview of macroautophagy regulation in mammalian cells. Cell Res. 2010;20(7):748-462. DOI: 10.1038/cr.2010.82.

43. Zhong P, Sun DM, Wu DH, Li TM, Liu XY, Liu HY. Serum total bilirubin levels are negatively correlated with metabolic syndrome in aged Chinese women: a community-based study. Braz J Med Biol Res. 2017;50(2):e5252,1-6.
DOI: 10.1590/1414-431X20165252.
44. Xu ZJ, Fan JG, Ding XD, Qiao L, Wang GL. Characterization of high-fat, diet-induced, non-alcoholic steatohepatitis with fibrosis in rats. Dig Dis Sci. 2010;55(4):931-940.
DOI: 10.1007/s10620-009-0815-3.
45. Takahashi Y, Fukusato T. Histopathology of nonalcoholic fatty liver disease/nonalcoholic steatohepatitis. World J Gastroenterol. 2014;20(42):15539-15548.
DOI: 10.3748/wjg.v20.i42.15539.
46. Salomone F, Li Volti G, Rosso C, Grosso G, Bugianesi E. Unconjugated bilirubin, a potent endogenous antioxidant, is decreased in patients with non-alcoholic steatohepatitis and advanced fibrosis. J Gastroenterol Hepatol. 2013;28(7):1202-1208.
DOI: 10.1111/jgh.12155.
47. McConnell MJ, Kostallari E, Ibrahim SH, Iwakiri Y. The evolving role of liver sinusoidal endothelial cells in liver health and disease. Hepatology. 2023;78(2):649-669.
DOI: 10.1097/HEP.0000000000000207.
48. Schepis F, Turco L, Bianchini M, Villa E. Prevention and management of bleeding risk related to invasive procedures in cirrhosis. Semin Liver Dis. 2018;38(3):215-229.
DOI: 10.1055/s-0038-1660523.
49. Preguica I, Alves A, Nunes S, Fernandes R, Gomes P, Viana SD, *et al*. Diet-induced rodent models of obesity-related metabolic disorders-a guide to a translational perspective. Obes Rev. 2020;21(12):e13081,1-29.
DOI: 10.1111/obr.13081.
50. Schroeder SM, Matsukuma KE, Medici V. Wilson disease and the differential diagnosis of its hepatic manifestations: a narrative review of clinical, laboratory, and liver histological features. Ann Transl Med. 2021;9(17):1394,1-16.
DOI: 10.21037/atm-21-2264.